



Modelling the Non-Linear Viscoelastic and Viscoplastic Behaviour of Aramid Fibre Yarns

E. CHAILLEUX and P. DAVIES

IFREMER (French Ocean Research Institute), Materials and Structures Group, Technopole de Brest-Iroise, B.P. 70, 29280 Plouzané, France; E-mail: peter.davies@ifremer.fr

(Received 9 July 2002; accepted 29 January 2003)

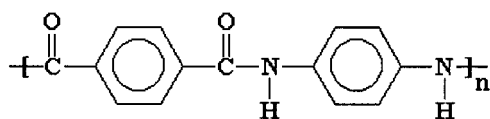
Abstract. A non-linear viscoelastic viscoplastic model is proposed for the tensile behaviour of aramid fibres, based on an analysis of the deformation mechanisms of these materials. This model uses the macroscopic formulation developed by Schapery together with the plasticity concept of Perzyna. A simple identification procedure for the model parameters has been developed using creep/recovery cycles at different load levels. The identification reveals that two of the four parameters of the viscoelastic model (g_1 and a_σ) are independent of stress level. This may be due to the simple and regular nature of the fibre structure. The model enables the parameters which characterise the non-linear reversible viscoelasticity to be identified independently from those which characterise the viscoplasticity. The model predictions are compared to experimental data for a more complex load sequence and reasonable correlation is obtained.

Key words: aramid, creep, fibre, viscoelastic, viscoplastic

1. Introduction

Synthetic fibre ropes are being used more and more widely in highly loaded applications (mooring lines for floating platforms, antenna guy ropes, etc.). The gain in weight and space associated with the use of polymer fibres has enabled steel cables to be replaced. However, the taut leg configuration rather than the catenary form commonly employed for steel cables, requires careful consideration to be given to the behaviour of these materials under static and cyclic loads over long periods. Although the geometry of the rope construction (such as braiding or twisting into strands) will have an influence on its mechanical behaviour it is the nature of the fibre which dominates creep and plastic strain (Davies et al., 2000). The analysis and modelling of the viscoelastic properties of synthetic fibres is therefore essential if long term performance of ropes is to be predicted accurately.

Aramid fibres (Twaron or Kevlar) have excellent properties (mechanical, thermal and chemical resistance (Yang, 1993)) and appear well suited for applications such as mooring lines provided compression loading can be avoided. Although they have highly oriented molecular structure creep and relaxation cannot be ignored when long lengths are subjected to long term loading (20 years or more for a floating offshore platform which may be moored in 3 kilometers water depth).



Several authors have worked on modelling of fibre behaviour previously. Baltussen and Northolt (2001), successfully applied a microscopic approach for creep (the 'continuous chain model'). That work showed that both the non-linear material response and plastic deformation must be taken into account. Lafitte and Bunsell (1985), modelled creep with a purely mathematical approach and concluded, like Baltussen, that creep strain could be described by a logarithmic expression. Secondary creep was shown to occur when the load exceeded 70% of the failure load. Wortmann and Schulz (2001) modelled relaxation behaviour using master curves and applying the theories of Schapery (Schapery, 1969). Analysis of the variations in relaxation times revealed that aramid fibres were 'more metallic than polymeric'.

2. Theoretical Part

2.1. MATERIAL

The material used in this study is an aramid fibre, Twaron 1000 (Teijin Twaron). The Twaron fibres, like Kevlar are aromatic polyamides (PPTA: poly(p-phenylene terephthalamide), see Figure 1). A characteristic of this type of molecule is that it can only exist in a 'trans' conformation. The bulky nature of the hydrogen atoms on the aromatic rings prevents rotation of the amides around the peptide groups, which can not take up a 'cis' conformation. In contrast to nylons, (which are also in the aramid family) the aromatic polyamide molecules can be perfectly extended. Thus these polymers can achieve a high degree of crystallinity as the phenyl groups in adjacent chains can stack up very easily and with a high degree of perfection. The adjacent macromolecular segments are held by hydrogen or Van Der Waal's bonds. As a result the molecular structure is very highly organised and the mechanical behaviour is very anisotropic. For these reasons the fibre is liable to fibrillate.

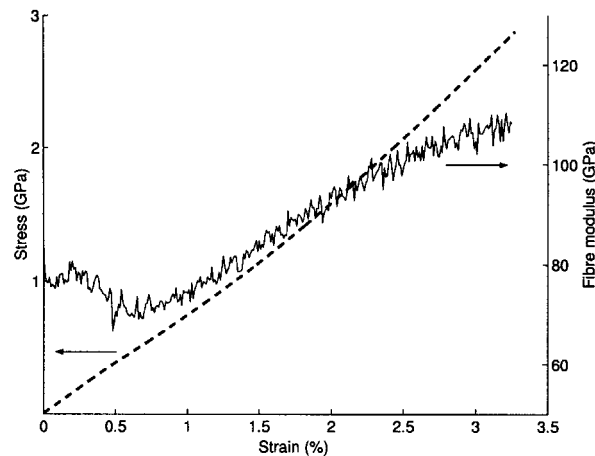


Figure 2. Stress-strain curve and modulus-strain curve for a Twaron1000 fibre.

2.2. MECHANISMS OF MOLECULAR DEFORMATION

The deformation mechanisms of aramid fibres have been studied in great detail by Northolt and colleagues (Northolt, 1980; Northolt and Sikkema, 1990; Northolt et al., 1995; Baltussen and Northolt, 1999). Their results show that the molecular alignment mechanism is responsible for the mechanical behaviour under tension loading. The observed strain is the result of the combined effects of the molecular elongation and the rotation of chains. An increase in tensile stress results in a stiffening of the fibre which can be observed experimentally (Figure 2). The rotation of the chains is made up of two components: one is reversible, the other is permanent and due to plastic deformation.

A model has been proposed (Northolt et al., 1995) enabling the plastic flow mechanism to be described and illustrating the importance of the initial orientation distribution of the molecules. The fibre is represented as an assembly of parallel domains of identical fibrils. Each fibril is a series of rectangular zones placed end to end. In each zone the polymer chains are parallel to each other but at an angle ϕ to the fibre axis (see Figure 3). For tensile loading, the maximum shear occurs in the zones with the largest angle and rotation will start in these zones. Increasing stress results in more and more zones with low angles to the fibre axis. As the orientation distribution reduces the fibre stiffness increases. The rotation of the zones is partially reversible, and on unloading the zones at the largest angles will define an angle to be reached before additional plastic deformation can occur. A fibre which has undergone tensile deformation will have an orientation distribution closer to the fibre axis and hence a higher tensile modulus. If the fibre is reloaded to a stress below the levels of previous loading there will be no further plastic strain mechanism. Figure 4 shows an example of this phenomenon. A fibre yarn (2000 filaments) has been successively loaded to different load levels. At each load creep strains followed by recovery are shown. It may be noted that the residual strain,

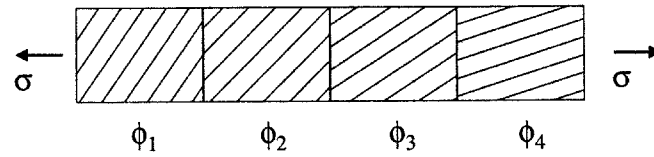


Figure 3. Schematic representation of a fibril by Northolt.

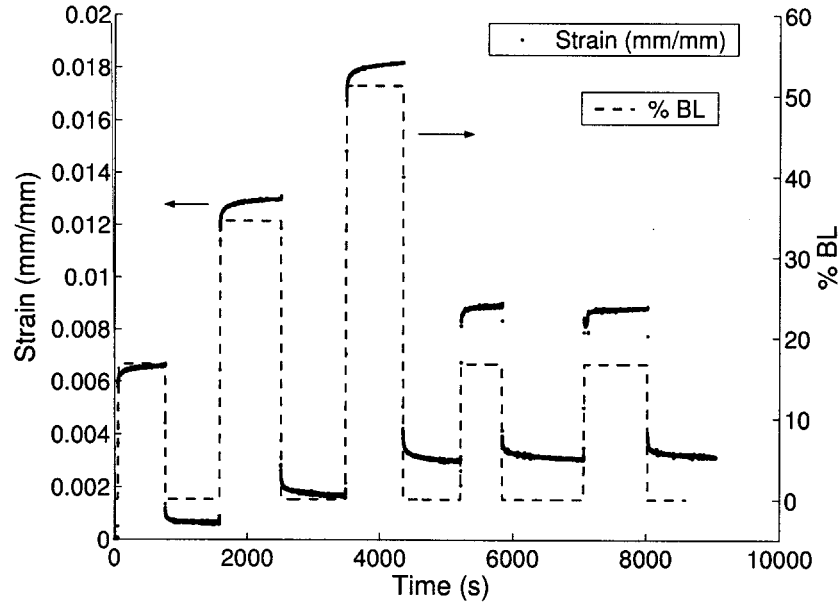


Figure 4. Cyclic loading of a Twaron 1000 yarn (BL: breaking load).

accumulated when the load increases, remains constant when the yarn is loaded to a load below that encountered previously.

The non-linear behaviour of these fibres is therefore the result of a sequential alignment mechanism of the macromolecular chains. This mechanism is also responsible for the plastic deformation. The covalent bonds only contribute to the elastic behaviour of the material (Yeh and Young, 1999). The shear deformations of the zones are the cause of the viscoelastic and viscoplastic deformation of the material through the secondary intermolecular bonds.

Based on these considerations it is possible to propose a separation of the overall strain into the different components (see Equation (1)) as a function of the molecular mechanisms. The strain is principally a result of the elongation and rotation of molecular chains: $\varepsilon_f = \varepsilon_{\text{stretch}} + \varepsilon_{\text{rotation}}$. The strain induced by chain rotation is made up of reversible and non-reversible contributions. The component $\varepsilon_{\text{stretch}} + \varepsilon_{\text{rev}}$ participates in the non-linear viscoelastic behaviour, depending on the time and the load level. The component ε_{irr} represents the viscoplastic behaviour of the material. It has been shown that the plastic strain is only accumulated when the flow criterion

$F \geq F_{\max}$ is satisfied. It depends therefore on the time, the current stress and the maximum stress previously seen by the fibre.

$$\varepsilon(t, \sigma) = \begin{cases} \varepsilon_{\text{stretch}}(\sigma) \\ + \\ \varepsilon_{\text{rotation}}(t, \sigma) \end{cases} \begin{cases} \varepsilon_{\text{rev}}(t, \sigma) \\ + \\ \varepsilon_{\text{irr}}(t, \sigma_y) \end{cases} \quad (1)$$

3. Modelling

As was indicated in Section 2.2, we will assume that the total strain can be divided up into a reversible part, related to the non-linear viscoelastic behaviour, and a non-reversible viscoplastic part.

$$\varepsilon(t) = \varepsilon_{\text{nlve}}(t) + \varepsilon_{\text{vp}}(t).$$

For the non-linear viscoelasticity the approach developed by Schapery (Lou and Schapery, 1971) will be applied. The viscoplastic strain will be expressed using Perzyna's (1966) approach.

3.1. NON-LINEAR VISCOELASTIC MODEL (SCHAPERY)

The single integral constitutive equation developed by Schapery is a macroscopic model based on thermodynamic assumptions. It enables the non-linear viscoelastic behaviour of materials to be described. For uniaxial loading under isothermal conditions, it may be written as follows:

$$\varepsilon_{\text{nlve}}(t) = g_0(\sigma) D_0 \sigma + g_1(\sigma) \int_0^t \Delta D(\Phi(t) - \Phi(\tau)) \frac{d(g_2(\sigma)\sigma)}{d\tau} d\tau. \quad (2)$$

In this expression, D_0 and $\Delta D(\Phi)$ are instantaneous and transient creep compliances. $\Phi(t)$ and $\Phi(\tau)$ are reduced times defined as

$$\Phi(t) = \int_0^t \frac{dt'}{a_\sigma} \quad \text{and} \quad \Phi(\tau) = \int_0^\tau \frac{d\tau'}{a_\sigma}.$$

a_σ is the acceleration factor. It describes coupling between stress and time for the creep compliance behaviour. The parameters g_0 , g_1 , g_2 , a_σ depend on the stress. They represent the non-linear material behaviour. Initially: $g_0(0) = g_1(0) = g_2(0) = a_\sigma(0) = 1$. It may be noted that for this special case the equation corresponds to Boltzmann's superposition principle and describes a linear viscoelastic material.

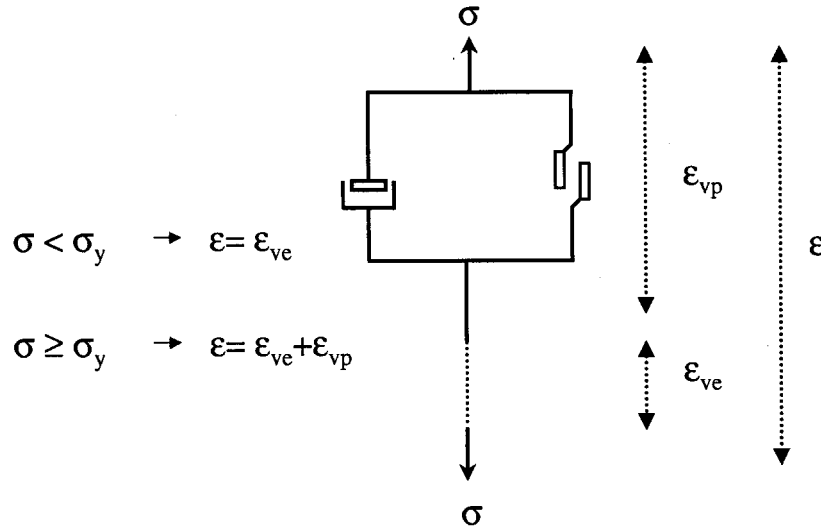


Figure 5. Perzyna's viscoplastic model.

3.2. PLASTICITY FUNCTION

The plasticity function is chosen to represent the material behaviour described in Section 2.2. The one-dimensional representation proposed by Perzyna (1966) appears well-suited to describe the viscoplastic strain behaviour of aramid fibres. In this model (see Figure 5), the viscoplastic response, which is simulated by a friction slider and a viscous damper, becomes effective as soon as the stress exceeds a characteristic value. This limit value is the current flow stress σ_y . The viscoplastic strain depends on the stress level with respect to σ_y and the application duration of the new load. This function differs from that applied by Lai and Bakker (1995) with polyethylene, for which this threshold is not observed.

We consider that the viscoplastic strain is a function of stress and time: $P(\sigma, t)$. It is also assumed that for multiple loadings

$$\sigma_1(t_1), \sigma_2(t_2), \dots, \sigma_i(t_i), \dots, \sigma_n(t_n),$$

the viscoplastic strain accumulates when $\sigma_i \geq \sigma_y$ and that the increment $\Delta \epsilon_p^i$ of viscoplastic strain resulting from the load σ_i for a time $\Delta t_i = t_{i+1} - t_i$ may be expressed as

$$\Delta \epsilon_{vp}^i = [P(\sigma_i, t_{i+1}) - P(\sigma_i, t_i)] + [P(\sigma_i, 0) - P(\sigma_y, 0)].$$

We then obtain

$$\epsilon_{vp}(t) = \epsilon_{vp}^n = \sum_{i=1}^n \phi \{ [P(\sigma_i, t_{i+1}) - P(\sigma_i, t_i)] + [P(\sigma_i, 0) - P(\sigma_y, 0)] \}, \quad (3)$$

with

$$\phi = \begin{cases} 0 & \text{if } \sigma < \sigma_y, \\ 1 & \text{if } \sigma \geq \sigma_y, \end{cases}$$

The flow stress σ_y is defined as follows: $\sigma_y = \max_{i=1}^n (\sigma_i)$.

4. Identification of Parameters

The non-linear viscoelastic viscoplastic model presented in the previous section must be adapted to the Twaron 1000 aramid fibres. It is therefore necessary to identify, from simple tests, the different parameters which characterise their behaviour. This identification is performed using tensile creep/recovery cycles at several load levels.

4.1. CREEP/RECOVERY FUNCTIONS

For creep, the strain expression, corresponding to a stress $\sigma = \sigma_c$ applied between $t = 0$ and $t = t_1$ may be written as

$$\varepsilon_c(t) = g_0 D_0 \sigma_c + g_1 g_2 \sigma_c \Delta D \left(\frac{t}{a_\sigma} \right) + P(\sigma_c, t). \quad (4)$$

The recovered strain when $\sigma = 0$ for $t > t_1$ is expressed as

$$\varepsilon_r(t) = g_2 \sigma_c \left(\Delta D \left(\frac{t_1}{a_\sigma} + t - t_1 \right) - \Delta D(t - t_1) \right) + P(\sigma_c, t_1).$$

However, in order to eliminate the residual strain $P(\sigma_c, t_1)$ from the expression for recovery, the relation used by Lai (Lai and Bakker, 1995): $\varepsilon_{cr} = \varepsilon_c(t_1) - \varepsilon_r(t)$, will be applied, i.e.,

$$\begin{aligned} \varepsilon_{cr}(t) = & g_0 D_0 \sigma_c \\ & + g_2 \sigma_c \left[g_1 \Delta D \left(\frac{t_1}{a_\sigma} \right) + \Delta D(t - t_1) - \Delta D \left(\frac{t_1}{a_\sigma} + t - t_1 \right) \right]. \end{aligned} \quad (5)$$

The results of Baltussen and Northolt (1999) and Lafitte and Bunsell (1985) show that the creep strain of aramid fibres follows a logarithmic law. Northolt and Sikkema (1990) attribute this logarithmic dependence to the fact that the structure of these fibres has a constant distribution of activation energies. The transient compliance can be represented as $\Delta D(t) = D_1 \log_{10}(t+1)$. D_1 corresponds to the creep rate. The plasticity function is also chosen so that it shows a logarithmic response: $P(\sigma, t) = \sigma(p + D_p \log_{10}(t+1))$ where p is the instantaneous component of the irreversible strain and where D_p corresponds to the plastic strain rate. Equations (4) and (5) can thus be written as

$$\varepsilon_c(t) = g_0 D_0 \sigma_c + g_1 g_2 \sigma_c D_1 \log_{10} \left(\frac{t}{a_\sigma} + 1 \right) + \sigma_c(p + D_p \log_{10}(t+1)), \quad (6)$$

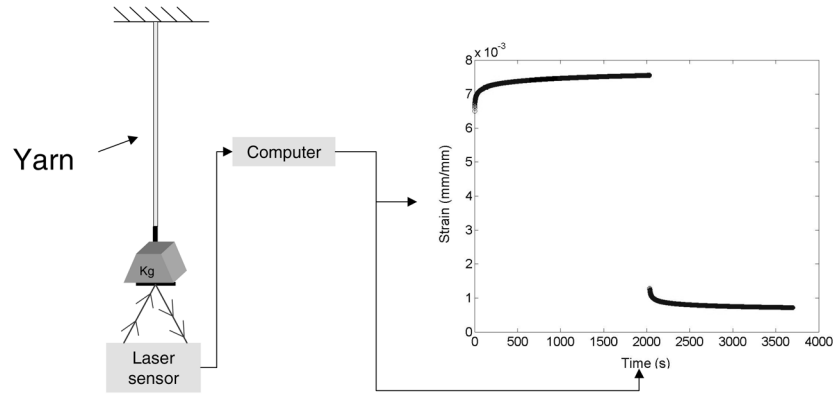


Figure 6. Schematic of the experimental setup.

$$\begin{aligned} \varepsilon_{cr}(t) = & g_0 D_0 \sigma_c + g_2 D_1 \sigma_c \left[g_1 \log_{10} \left(\frac{t_1}{a_\sigma} + 1 \right) \right. \\ & \left. + \log_{10}(t - t_1 + 1) - \log_{10} \left(\frac{t_1}{a_\sigma} + t - t_1 + 1 \right) \right]. \end{aligned} \quad (7)$$

4.2. EXPERIMENTAL CONDITIONS

The study of the mechanical behaviour of single fibres showed considerable variability in the results. The reproducibility of measurements at this scale is complicated by the heterogeneous nature of the fibres and by the measurement difficulties resulting from the very low loads required to load single fibres in tension. For these reasons, tests were performed to characterise the material at the yarn level, a yarn consisting of 2000 filaments. The averaging effect of testing 2000 fibres allowed satisfactory reproducibility to be obtained in tension and tensile creep tests. Stress is calculated based on average fibre diameter (from electron microscope observation: $12 \mu\text{m}$).

An experimental set-up was developed in order to measure the creep and recovery strains. The main difficulty is to measure small displacements accurately without contact, as fixing an extensometer to the yarn would impede recovery measurements. The approach employed was to suspend long lengths, 2500 mm long, and to fix a support to the lower end to take the weights. The displacement is obtained from a laser displacement transducer, using triangulation and capable of detecting movements of less than 10 microns of a reflector fixed to the central axis of the support. The tests were performed in a controlled environment laboratory at $20^\circ\text{C} \pm 1^\circ\text{C}$. A schematic illustration of the set-up is shown in Figure 6. Strain data were stored digitally for subsequent analysis.

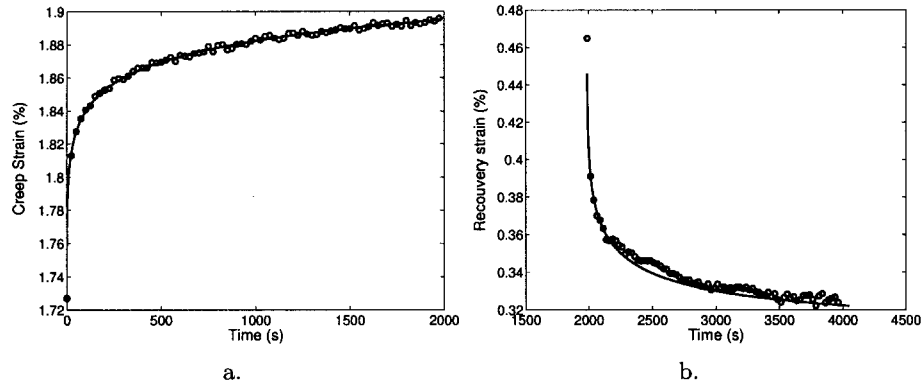


Figure 7. Creep and recovery strain. Circles: experimental. continuous line: model.

4.3. MULTI-VARIABLE OPTIMISATION

The parameters are obtained by fitting the theoretical curves to the experimental data of $\varepsilon_{cr}(t)$ and $\varepsilon_c(t)$. Fitting is performed using unconstrained non-linear optimisation algorithms in the least squares sense. First, a simplex method is used in order to approach the solution. Then, refined results are determined using an interior-reflective Newton method.

The multi-variable optimisation is first performed on the parameters concerning $\varepsilon_{cr}(t)$, i.e., $A_0 = g_0 D_0$, $A_1 = g_2 D_1$, a_σ , g_1 . Then taking into account the results of this first step, the optimisation procedure is applied to the parameters of the plasticity function concerning $\varepsilon_c(t)$. This method enables the viscoelastic and viscoplastic parameters to be determined independently. Also, the parameters a_σ and g_1 were found to be independent of the load. The optimisation was therefore performed for $a_\sigma = 1$ and $g_1 = 1$. The single phase, regular structure of these fibres could explain the invariance of a_σ . This result also indicates that the time-stress superposition principle cannot be applied to aramid fibres.

This procedure was applied for six stress levels, using a new length of yarn for each test, at loads up to 50% of the quasi-static failure load of the yarn, i.e. up to $F_{max} = 300$ N. Figures 7a and 7b present the result of an optimisation for a creep/recovery cycle at 300N. The theoretical curves fit well to the experimental points, justifying the choice of transient creep and plasticity functions used in Equations (6) and (7).

4.4. INTERPOLATION – EVOLUTION OF PARAMETERS AS A FUNCTION OF APPLIED LOAD

Three tests were performed at each load level. The evolution of the parameters $A_0 = g_0 D_0$, $A_1 = g_2 D_1$, p and Dp calculated by optimisation are then extrapolated by polynomial functions (see Figures 8a, 8b, 9a and 9b). It should be noted

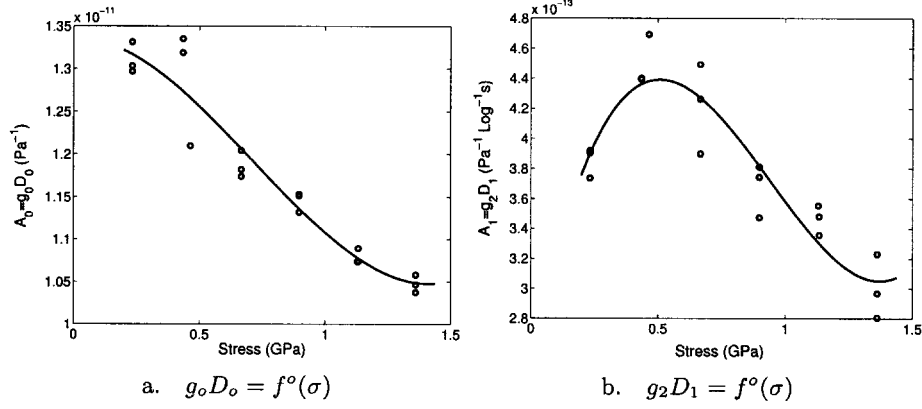


Figure 8. Non-linear viscoelastic parameters as a function of stress. Circles: from optimisation. Continuous line: polynomial extrapolation.

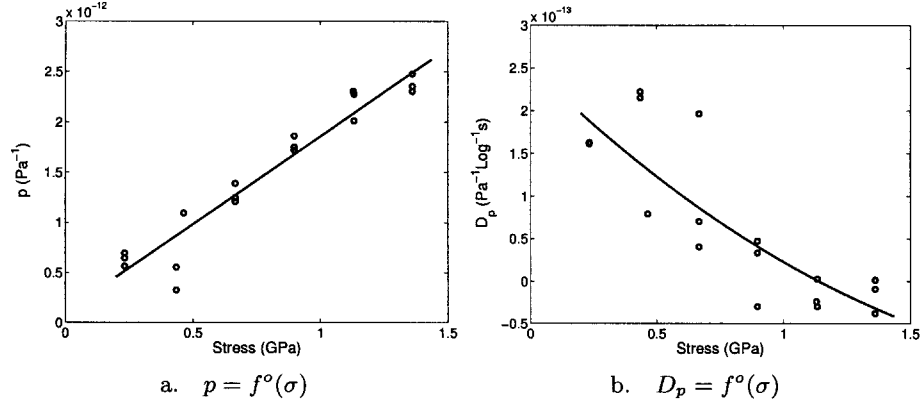


Figure 9. Viscoplastic parameters as a function of stress. Circles: from optimisation. Continuous line: polynomial extrapolation.

that g_0 , D_0 , g_2 and D_1 can be determined independently. Then by extrapolating A_0 and A_1 for $\sigma = 0$ where $g_0 = g_2 = 1$, the values D_0 and D_1 can be found. In the present study, only the evolution of the parameters A_0 and A_1 was analysed.

The instantaneous compliance A_0 decreases with stress from $1.32 \cdot 10^{-11}$ to $1.05 \cdot 10^{-11} \text{ Pa}^{-1}$. The non-linear nature of the material is therefore dominated by the instantaneous response. The instantaneous moduli (deduced from $E_0 = 1/A_0$ and $E_1 = 1/A_1$), increase with load from 75 to 95 GPa. These values are similar to those obtained in a quasi-static tensile test on a single fibre (see Figure 2). The creep rate A_1 also shows non-linear behaviour. It shows a maximum for $\sigma = 0.5 \text{ GPa}$, then decreases at 1.4 GPa from $4.4 \cdot 10^{-13}$ to $3 \cdot 10^{-13} \text{ Pa}^{-1} \log^{-1} \text{ s}$.

The parameter p representing the instantaneous plasticity increases linearly with the stress. However, the plastic strain rate D_p tends to zero when the stress increases. At 50% of the failure stress, the viscoplasticity of the fibres occurs in-

stantaneously and does not evolve further with time. The creep strain is then only the result of reversible alignment of molecular chains.

5. Model – Test Comparison

The strain of the yarn subjected to any tensile loading/unloading sequence is calculated from Equations (2) and (3). We consider a discrete loading history $\sigma_0, \sigma_1, \dots, \sigma_i, \dots, \sigma_n$ starting respectively at times $0 < t_1 < t_2 < \dots t_i < \dots t_n$. The non-linear viscoelastic and viscoplastic strains for the n th loading are written as

$$\begin{aligned} \varepsilon_{nlve}^n = & A_0(\sigma_n)\sigma_n + g_1(\sigma_n) \sum_{i=1}^{i=n} \log \left(\sum_{k=i}^{k=n} \left(\frac{t_{k+1} - t_k}{a_\sigma(\sigma_k)} \right) + 1 \right) \\ & \times (A_1(\sigma_i)\sigma_i - A_1(\sigma_{i-1})\sigma_{i-1}), \end{aligned} \quad (8)$$

$$\varepsilon_p^n = \sum_{i=1}^n \phi \left\{ \sigma_i Dp(\sigma_i) \log \left(\frac{t_{i+1} + 1}{t_i + 1} \right) + [\sigma_i p(\sigma_i) - \sigma_y p(\sigma_y)] \right\}. \quad (9)$$

The parameters A_0 , A_1 , D_p and p are obtained for each loading from their polynomial extrapolations (see Figures 8a, 8b, 9a and 9b). The loading profile shown in Figure 4 is used to check the validity of the model. The predicted strains are compared with measurements in Figure 10. The theoretical curve shows a satisfactory correlation with the measured strains. The plastic strain after the third loading (to 50 % breaking load) is slightly overestimated, and this error influences the subsequent load cycle results. However, overall the deformation mechanisms are reasonably well accounted for. Viscoplastic strain is accumulated only when the fibre is subjected to a load higher than that previously encountered. The non-linearity is also modelled and the model takes the loading history into account. The first and last load cycles are identical but the strain responses are different. Between the two cycles stiffening and plasticisation of the fibre have taken place. It may be noted that the validation test duration is 2.5 hours while identification test lasted only one hour.

6. Conclusion

A non-linear viscoelastic viscoplastic model is proposed for the tensile behaviour of aramid fibres, based on an analysis of the deformation mechanisms of these materials. This model uses the macroscopic formulation developed by Schapery together with the plasticity concept of Perzyna. A simple identification procedure for the model parameters has been developed using creep/recovery cycles at different load levels. The identification reveals that two of the four parameters of the viscoelastic model (g_1 and a_σ) are independent of stress level. This may be due to

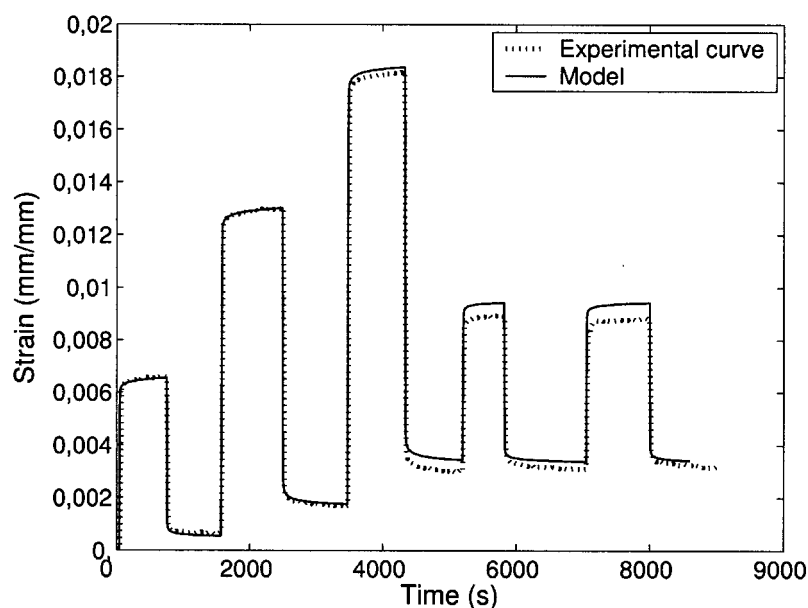


Figure 10. Experimental result/model comparison.

the simple and regular nature of the fibre structure. The model enables the parameters which characterise the non-linear reversible viscoelasticity to be identified independently from those which characterise the viscoplasticity. The model predictions are compared to experimental data for a more complex load sequence and reasonable correlation is obtained. This suggests that the model could be applied in a design tool for predicting the mechanical behaviour of fibre ropes subjected to long term loading. Further work is underway to examine whether this type of model is applicable to ropes based on other fibre materials (polyester, high modulus polyethylene, PBO, etc.). Work is also underway to examine in more detail the physical significance of the model parameters, in order that the polynomial extrapolation functions used to represent viscoelastic and viscoplastic evolution might be replaced by functions based on macromolecular deformation mechanisms.

Acknowledgements

The authors thank Dr. Grabandt (Twaron) for the gift of material. The technical expertise of Luc Riou (IFREMER) is also gratefully acknowledged.

References

- Baltussen, J.J.M. and Northolt, M.G., 'The stress and sonic modulus versus strain curve of polymer fibres with yield', *Polymer* **40**, 1999, 6113–6124.
- Baltussen, J.J.M. and Northolt, M.G., 'The viscoelastic extension of polymer fibres: creep behaviour', *Polymer* **42**, 2001, 3835–3846.

- Davies, P., Huard, G., Grosjean, F. and François, M., 'Creep and relaxation of polyester mooring lines', in *Proceedings of the Offshore Technology Conference*, 2000, Paper OTC 12176, 1–12.
- Dillard, D.A., *Fatigue of Composite Materials*, Composite Materials Series, Vol. 4, Elsevier, Amsterdam, 1991, 339–384.
- Lafitte, M.H. and Bunsell, A.R., 'The creep of Kevlar-29 fibers', *Polymer Engineering and Science* **25**(3), 1985, 182–187.
- Lai, J. and Bakker, A., 'An integral constitutive equation for nonlinear plasto-viscoelastic behaviour of high-density polyethylene', *Polymer Engineering and Science* **35**(17), 1995, 1339–1347.
- Lou, Y.C. and Schapery, R.A., 'Viscoelastic characterisation of a nonlinear fiber-reinforced plastic', *Journal of Composite Materials* **5**(18), 1971, 208–234.
- Northolt, M.G., 'Tensile deformation of poly(p-phenylene terephthalamide) fibres, an experimental and theoretical analysis', *Polymer* **21**, 1980, 1199–1203.
- Northolt, M.G. and Sikkema, D.J., 'Lyotropic main chain liquid crystal polymers', *Advances in Polymer Science* **98**, 1990, 115–176.
- Northolt, M.G., Baltussen, J.J.M. and Schaffers-Korff, B., 'Yielding and hysteresis of polymer fibres', *Polymer* **36**(18), 1995, 3485–3492.
- Perzyna, P., 'Fundamental problems in viscoplasticity', *Advances in Applied Mechanics* **9**, 1966, 243–377.
- Schapery, R.A., 'On the characterization of nonlinear viscoelastic materials', *Polymer Engineering and Science* **9**, 1969, 295–310.
- Schapery, R.A., 'Nonlinear viscoelastic and viscoplastic constitutive equations based on thermodynamics', *Mechanics of Time-Dependent Materials* **1**, 1997, 209–240.
- Wortmann, F.J. and Schulz, K.V., 'Non-linear viscoelastic performance of Nomex, Kevlar and polypropylene fibres in a single step stress relaxation test: 2. Moduli, viscosities and isochronal stress/strain curves', *Polymer* **36**(12), 2001, 2363–2369.
- Yang, H.H., *Kevlar Aramid Fiber*, John Wiley and Sons, New York, 1993.
- Yeh, W.Y. and Young, R.J., 'Molecular deformation processes in aromatic high modulus polymer fibres', *Polymer* **40**, 1999, 857–870.
- Zaoutos, S.P., Papanicolaou, G.C. and Cardon, A.H., 'On the non-linear viscoelastic behaviour of polymer-matrix composites', *Composites Science and Technology* **58**, 1998, 883–889.